Proceedings of "Applications of Physics in Mechanical and Material Engineering" (APMME 2023)

The Influence of the Shape of Acoustic Impedance Change on the Propagation of a Mechanical Wave in Multilayer Phononic Structures

S. Garus*

Department of Mechanics and Fundamentals of Machinery Design, Faculty of Mechanical Engineering and Computer Science, Czestochowa University of Technology, Dąbrowskiego 73, 42-201 Częstochowa, Poland

Doi: 10.12693/APhysPolA.144.313 *e-mail: sebastian.garus@pcz.pl

Thanks to the use of modern intelligent materials, such as composites consisting of piezoceramic fibers embedded in epoxy resin and covered with alternating electrodes, electroactive polymers, dielectric elastomers, magnetostrictive composites with epoxy resin or ferromagnetic alloys with shape memory, it is possible to control the geometry or properties of materials using pressure, external magnetic or electric fields. The paper analyzes multilayer quasi-one-dimensional phononic structures in which the selected layer is made of a material with time-varying acoustic impedance. The influence of the shape of the material properties changes over time (square wave, triangle wave, sawtooth wave) on the propagation of mechanical waves in the structure is analyzed.

topics: mechanical wave, finite difference time domain (FDTD), propagation, multilayers

1. Introduction

Many studies have been carried out describing the usefulness of phononic crystals as acoustic barriers [1], waveguides [2, 3], mechanical wave filters [4–7], acoustic diodes [8], or sensors [9]. One of the most interesting phenomena occurring during wave propagation in multilayer structures is the presence of a phononic band gap (PhnBG). Despite many years of research on PhnBG, many authors continue to develop this research and obtain interesting results [10–13].

The latest trends in the study of phononic crystals concern structures that can be "steerable." The building blocks of such crystals may be composite materials consisting of layered piezoceramic fibers embedded in epoxy resin and covered with electrodes [14, 15], magnetostrictive composites [16, 17], electroactive polymers (EAP) [18, 19], ferroelectric shape memory alloys [20], or carbon nanotubes [21].

The work analyzed the influence of changing the shape of the material parameters on the propagation of a mechanical wave in a multilayer structure.

2. Research

The propagation of a mechanical wave is described by differential equations

$$\frac{\partial P_{x,y,z,t}}{\partial t} = \rho_{x,y,z,t}\, c^2_{x,y,z,t}\, \nabla \cdot \boldsymbol{v}_{x,y,z,t}, \tag{1}$$

$$\rho_{x,y,z,t}\, c_{x,y,z,t} \frac{\partial \boldsymbol{v}_{x,y,z,t}}{\partial t} = \nabla P_{x,y,z,t}, \tag{2}$$

where $P_{x,y,z,t}$ is a scalar pressure field determined in time t and Euclidean space (x, y, z); $\rho_{x,y,z,t}$ and $c_{x,y,z,t}$ describe the material parameters (mass density and phase velocity, respectively), which for layer B are variable in time t; $\boldsymbol{v}_{x,y,z,t}$ is a vector of the velocity field.

By transforming equations (1) and (2) into a form describing a quasi-one-dimensional space in a form adapted to the finite difference algorithm in the time domain (FDTD), we obtained

$$P_x^{t+1/2} = P_x^{t+1/2} + C\, \rho_{x,t} c^2_{x,t} \left(v^t_{x+1/2} - v^t_{x-1/2} \right) \tag{3}$$

$$v^{t+1}_{x+1/2} = v^t_{x+1/2} + C \frac{1}{\rho_{x,t}} \left(P^{t+1/2}_{x+1} - P^{t+1/2}_{x} \right), \tag{4}$$

where

$$C = \frac{\Delta t}{\Delta z}. \tag{5}$$

The steps in time Δt and space Δz that ensure simulation stability are related to the Courant condition via

$$\Delta t \leq \frac{\Delta z}{c_{\max}}, \tag{6}$$

where $c_{\max}$ is the highest possible speed of mechanical wave propagation in the structure.

The paper analyzed the propagation of a mechanical wave in the BABAB structure. The material of the A layers and the surrounding material

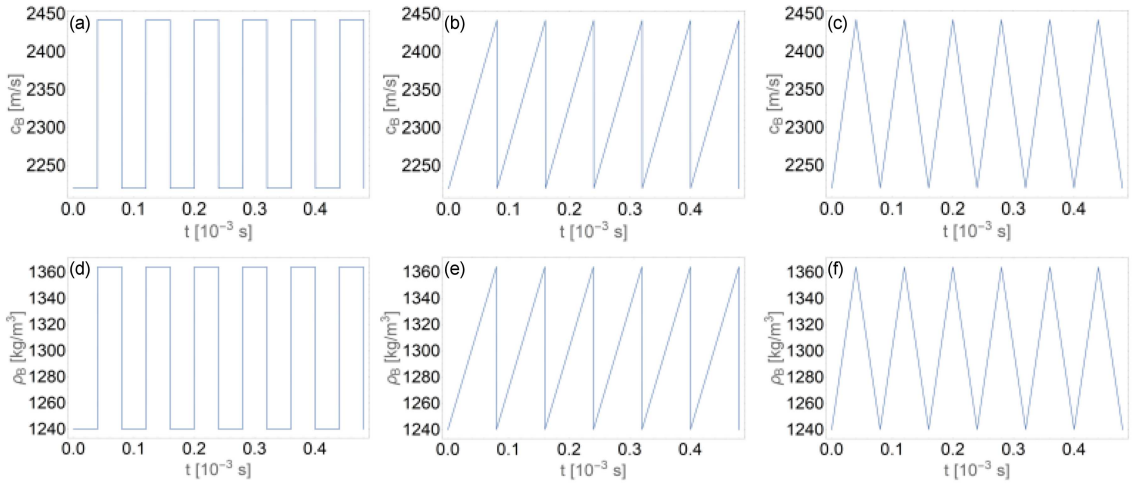

Fig. 1. Change in material parameters of layer B over time with (a, d) square, (b, e) sawtooth, and (c, f) triangle shape.

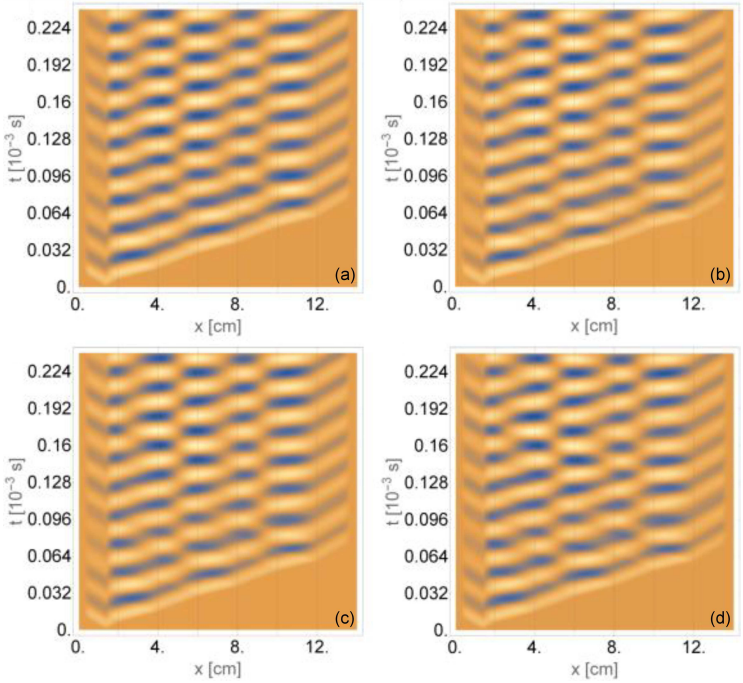

Fig. 2. Pressure distribution in time and space for changing material parameters of layer B with (a) solid, (b) triangle, (c) sawtooth, and (d) square shape.

was water, for which the assumed values of the material parameters were $\rho_A = 1000$ kg/m^3 and $c_A = 1480$ m/s [22]. In turn, material B was a material with time-varying properties, for which the basic values were the material parameters suitable for polylactic acid (PLA) ($\rho_B = 1240$ kg/m^3 and $c_B = 2220$ m/s [23]), which varied over time between the minimum value of material parameters corresponding to those suitable for PLA and the maximum values that were 10% higher than the base values. Changes in the values of material parameters over time are shown in Fig. 1.

The work used a soft mechanical wave source, and the simulation was surrounded by perfectly matched layer (PML) boundary conditions in order to extinguish the wave at the simulation boundary. In the tests, the frequency of the mechanical wave source was assumed to be 40 kHz, the thickness of the individual layers was 2 cm, the maximum assumed phase velocity of the mechanical wave was 5000 m/s, the step in space was $\Delta z = 0.4 \times 10^{-3}$ m, and the step in time was $\Delta t = 8 \times 10^{-8}$ s. The period of changes in the values of material parameters presented in Fig. 1 was $T = 80 \times 10^{-6}$ s. The analysis was performed for 10^4 time steps.

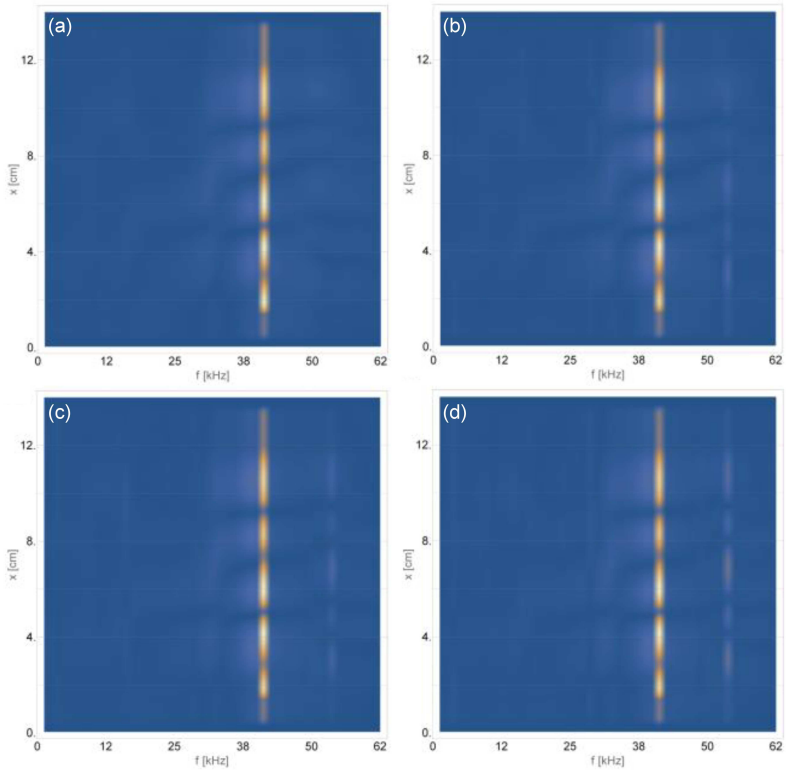

Fig. 3. Distribution of local resonance fields for changing the material parameters of layer B with (a) solid, (b) triangular, (c) sawtooth, and (d) square shape.

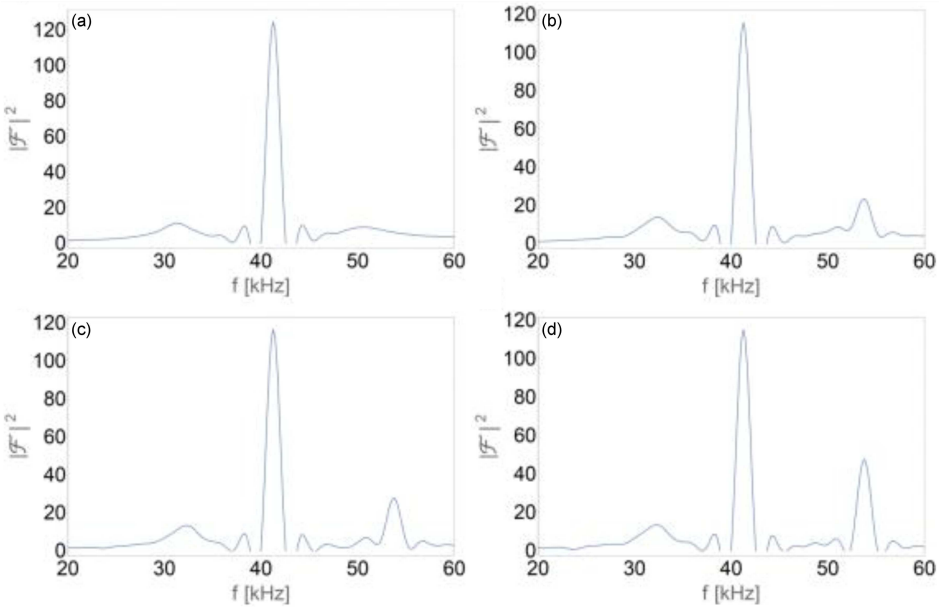

Fig. 4. Fourier transforms of signals occurring at the midpoint of the analyzed structure for changing the material parameters of layer B with (a) solid, (b) triangular, (c) sawtooth, and (d) square shape.

Figure 2 shows the pressure distribution in time and space for the first 3000 time steps. Figure 2a shows the results for a material with constant parameters suitable for PLA, while Fig. 2b–d shows the results for changes in material parameters in the (b) triangle, (c) sawtooth, and (d) square shape. As can be seen in Fig. 2a, when the wave reflected from the last boundary of the media reaches the first boundary of the media, a stable system of standing waves is created inside the phononic structure. Dynamically changing values of the material parameters of layers B (Fig. 2b–d) destabilize the rapid

formation of standing waves inside the multilayer structure. Maximum pressure changes occur at the boundaries of the centers. The longest stabilization time of standing waves inside the structure occurred for changes in material parameters with a square shape.

Figure 3 shows the intensity of frequencies occurring in the analyzed space. In all analyzed cases, there was a peak related to the frequency of the mechanical wave source. When introducing changes in the material properties over time (Fig. 3b–c), an additional peak was created in the wave spectrum at the frequency 53.75 kHz. The spectrum of the signal from the central point of the structure is also shown in Fig. 4. As can be seen, the intensity of the peak was related to the shape of changes in the material parameters of layer B and was the highest for the square shape (Fig. 4d), and then increasingly lower for the sawtooth (Fig. 4c) and triangular (Fig. 4b) shape. The energy introduced into the system is proportional to the square of the amplitude of material changes and is highest for the square shape, where the highest peak intensity occurs.

3. Conclusions

As part of the research, the influence of the shape of changes in material parameters of layers B of a multilayer structure on the propagation of a mechanical wave inside the structure was analyzed.

The introduction of additional energy in the form of changes in the material parameters of layer B resulted in a slowdown in the process of creating standing waves inside the structure and the creation of an additional peak in the frequency distribution inside the multilayer structure. The highest intensity of the obtained peak occurred for square-shaped material changes and was associated with the highest amount of energy introduced into the system.

References

[1] J.V. Sanchez-Perez, C. Rubio, R. Martinez-Sala, R. Sanchez-Grandia, V. Gomez, *Appl. Phys. Lett.* **81**, 5240 (2002).

[2] J. Wen, D. Yu, L. Cai, X. Wen, *J. Phys. D: Appl. Phys.* **42**, 115417 (2009).

[3] B. Morvan, A. Tinel, J.O. Vasseur, R. Sainidou, P. Rembert, A.-C. Hladky-Hennion, N. Swinteck, P.A. Deymier, *J. Appl. Phys.* **116**, 214901 (2014).

[4] W. Sochacki, *Acta Phys. Pol. A* **138**, 328 (2020).

[5] S. Villa-Arango, R. Torres, P.A. Kyriacou, R. Lucklum, *Measurement* **102**, 20 (2017).

[6] C.J. Rupp, M.L. Dunn, K. Maute, *Appl. Phys. Lett.* **96**, 111902 (2010).

[7] S. Garus, W. Sochacki, *Wave Motion* **98**, 102645 (2020).

[8] X.-F. Li, X. Ni, L. Feng, M.-H. Lu, C. He, Y.-F. Chen, *Phys. Rev. Lett.* **106**, 084301 (2011).

[9] S. Garus, *Rev. Chim.* **70**, 3671 (2019).

[10] W. Witarto, K.B. Nakshatrala, Y-L. Mo, *Mech. Mater.* **134**, 38 (2019).

[11] Y.F. Li, F. Meng, S. Li, B. Jia, S. Zhou, X. Huang, *Phys. Lett. A.* **382**, 10, 679 (2018).

[12] E. Li, Z.C. He, G. Wang, *Comput. Mater. Sci.* **122**, 72 (2016).

[13] S-L. Cheng, J-M. Liang, Q. Ding, Q. Yan, Y-T. Sun, T-J. Xin, L. Wang, *Wave Motion* **122**, 103195 (2023).

[14] M. Melnykowycz, X. Kornmann, C. Huber, M. Barbezat, A.J. Brunner, *Smart Mater. Struct.* **15**, 204 (2006).

[15] R. Paradies, P. Ciresa, *Smart Mater. Struct.* **18**, 035010 (2009).

[16] S. Levgold, J. Alstad, J. Rhyne, *Phys. Rev. Lett.* **10**, 509 (1963).

[17] C. Rodrígueza, M. Rodrigueza, I. Oruec, J.L. Vilas, J.M. Barandiaránb, M.L.F. Gubiedab, L.M. Leona, *Sens. Actuators A* **149** 251 (2009).

[18] W-P. Yang, L-W. Chen, *Smart Mater Struct.* **17**, 015011 (2008).

[19] J-S. Plante, S. Dubowsky, *Smart Mater. Struct.* **16**, 227 (2007).

[20] Y. Ganora, D. Shilo, J. Messier, T.W. Shield, R.D. James, *Rev. Sci. Instrum.* **78**, 073907 (2007).

[21] A.E. Aliev, J. Oh, M.E. Kozlov, A.A. Kuznetsov, S. Fang, A.F. Fonseca, R. Ovalle, M.D. Lima, M.H. Haque, Y.N. Gartstein, M. Zhang, A.A. Zakhidov, R.H. Baughman, *Science* **323**, 1575 (2009).

[22] Y. Wang, W. Song, E. Sun, R. Zhang, W. Cao, *Physica E* **60**, 37 (2014).

[23] D. Tarrazó-Serrano, S. Castiñeira-Ibáñez, E. Sánchez-Aparisi, A. Uris, C. Rubio, *Appl. Sci.* **8**, 2634 (2018).